Supporting Information

Unraveling Defect-Mediated Ion Transport Behavior in Anti-Perovskite Solid-State Electrolyte via Machine Learning Molecular Dynamics Simulations

Lirong Xia[a], *Kehao Zhang*[a], *Yong Pei**[a]

[a]Department of Chemistry, Key Laboratory of Environmentally Friendly Chemistry and Applications of Ministry of Education, Xiangtan University, Xiangtan 411105, P. R. China;

***Corresponding Authors:** ypei2@xtu.edu.cn (Y. P.)

1. More details of simulations and calculations.

1.1 The error validation of the DP model.

To evaluate the accuracy of the trained DP model, firstly, we performed 200 fs AIMD simulations on the eight structures shown in **Figure 1** at temperatures ranging from 300 to 900 K (in 100 K increments). Then, we randomly selected 100 data points from the AIMD simulation trajectories of each of the eight systems to form the test set. **Figures S1** and **S2** show a comparison of the energy and force predicted by the DP model and DFT calculation. It is evident that for all systems (including perfect and defective ones), the energy and force are well distributed along the diagonal, with R^2 values greater than 0.99. Additionally, for all systems, the energy and force errors are as low as 10^{-4} eV/atom and 10^{-2} eV/Å, respectively.

In addition, to verify the reliability of the DP model under extreme structural deformation, we collected all configurations generated during iterative DPGEN sampling and compared the energy and force calculated by DFT and predicted by DP.

As shown in **Figure S3**, the model achieves excellent agreement across both low- and high-temperature regions, with energy and force errors of 1.05×10^{-3} eV/atom and 2.41×10^{-2} eV/Å, respectively. Notably, configurations with severe Li_6O octahedral distortion and low-coordinated Li-O polyhedra are also accurately predicted, confirming its capability to reliably describe extreme disordered states.

1.2 Defect reaction equation.

Li_2O-Schottky pair ($2V_{Li}^{'} - V_O^{\bullet\bullet}$) :

$$2Li_{Li}^{\times} + O_O^{\times} \rightarrow 2V_{Li}^{'} + V_O^{\bullet\bullet} + Li_2O\#(S1)$$

LiCl-Schottky pair ($V_{Li}^{'} - V_{Cl}^{\bullet}$) :

$$Li_{Li}^{\times} + Cl_{Cl}^{\times} \rightarrow V_{Li}^{'} + V_{Cl}^{\bullet} + LiCl\#(S2)$$

O-Cl substitution ($Li_i^{\bullet} + O_{Cl}^{'}$):

$$Li_2O + Cl_{Cl}^{\times} \rightarrow Li_i^{\bullet} + O_{Cl}^{'} + LiCl\#(S3)$$

LiCl-Schottky + Li_2O-Schottky:

$$3Li_{Li}^{\times} + O_O^{\times} + Cl_{Cl}^{\times} \rightarrow 3V_{Li}^{'} + V_O^{\bullet\bullet} + V_{Cl}^{'} + Li_3OCl\#(S4)$$

LiCl-Schottky + O-Cl substitution:

$$Li_2O + 2Cl_{Cl}^{\times} \rightarrow V_{Cl}^{\bullet} + O_{Cl}^{'} + 2LiCl\#(S5)$$

Li_2O-Schottky + O-Cl substitution:

$$Li_{Li}^{\times} + O_O^{\times} + Cl_{Cl}^{\times} \rightarrow O_{Cl}^{'} + V_O^{\bullet\bullet} + V_{Li}^{'} + LiCl\#(S6)$$

1.3 Defect formation energy and binding energy.

The binding energy of a defect pair reflects the thermodynamic stability of the paired defect relative to isolated defects. For example, the binding energy of a LiBr-Schottky defect measures the strength of binding between a Li vacancy and a Br vacancy. The larger the binding energy, the stronger the binding capability of the Br vacancy to the Li vacancy. [1] Consequently, in systems with high defect binding energies, the anion vacancies act as effective scattering centers that hinder the migration

of adjacent Li vacancies and elevate the local energy barriers for diffusion.[2] This scattering effect disrupts the formation of continuous diffusion pathways, resulting in more localized ionic motion. The calculation formula for defect formation energy (E_f) is as follows:

$$E_f = E_{defect} - E_{pefect} - \sum n_i \mu_i \#(S7)$$

Where E_{pefect} represents the energy of the perfect system, E_{defect} represents the energy of the defective system, n_i and μ_i represent the number of defective atoms and the corresponding chemical potential, respectively. The binding energy of the defect pair is calculated by the following formula[1]:

$$E_{binding} = \sum E_{isolate\ defect} - E_{cluster}\ \#(S8)$$

Where $E_{binding}$ represents the binding energy of the defect pair, while $E_{isolate\ defect}$ and $E_{cluster}$ represent the formation energies of the individual defect and the defect pair, respectively.

2. Supplementary table

Table S1 Parameter settings for the DGPEN iterative process. N_{steps}, N_{dft}, and Accurate represent the steps of DPMD simulations in the iterative process, the number of DFT single-point calculations, and the accuracy, respectively.

Iteration	Ensemble	Temperature (K)	Pressure (bar)	Structure	N_{steps} (fs)	N_{dft}	Accurate(%)
0	NPT	300, 500, 700,900	0.1, 5, 10, 100	a	5000	300	95.57
1	NPT	300, 500, 700,900	0.1, 5, 10, 100	b	8000	300	95.27
2	NPT	300, 500, 700,900	0.1, 5, 10, 100	c	8000	300	78.34
3	NPT	300, 500, 700,900	0.1, 5, 10, 100	d	8000	96	99.96
4	NPT	300, 500, 700,900	0.1, 5, 10, 100	e	8000	300	97.89
5	NPT	300, 500, 700,900	0.1, 5, 10, 100	f	8000	300	99.78
6	NPT	300, 500, 700,900	0.1, 5, 10, 100	j	8000	1	100.00
7	NPT	300, 500, 700,900	0.1, 5, 10, 100	h	8000	33	99.99
8	NVT	300, 500, 700,900	0.1, 5, 10, 100	a	6000	0	100.00
9	NVT	300, 500, 700,900	0.1, 5, 10, 100	b	10000	0	100.00
10	NVT	300, 500, 700,900	0.1, 5, 10, 100	c	10000	9	99.98
11	NVT	300, 500, 700,900	0.1, 5, 10, 100	d	10000	4	99.99
12	NVT	300, 500, 700,900	0.1, 5, 10, 100	e	10000	73	99.80
13	NVT	300, 500, 700,900	0.1, 5, 10, 100	f	10000	4	99.99
14	NVT	300, 500, 700,900	0.1, 5, 10, 100	j	10000	1	100.00
15	NVT	300, 500, 700,900	0.1, 5, 10, 100	h	10000	5	99.99

Table S2 Diffusion coefficients of Li_3OCl systems with different defects

T **(K)**	***D*** **(cm^2/s)**					
	Type 1	Type 2	Type 3	Type 12	Type 13	Type 23
300	2.08E-9	2.79E-9	-	1.06E-8	-	6.23E-9
400	9.19E-9	7.18E-9	-	5.64E-8	-	7.94E-9
500	4.74E-8	3.65E-8	9.25E-9	2.98E-7	-	1.73E-8
600	1.27E-7	1.86E-7	6.10E-8	2.07E-6	-	4.64E-8
700	2.26E-7	1.23E-6	2.13E-7	7.50E-6	5.41E-9	1.97E-7
800	4.01E-7	1.82E-5	5.39E-7	1.70E-5	8.44E-9	2.31E-6
900	1.24E-6	3.13E-5	1.14E-6	2.91E-5	4.97E-7	2.93E-5

Table S3 Defect binding energy

Type	Binding energy (eV)
Type 1	-0.134
Type 2	0.207
Type 3	0.735

3. Supplemental Figures

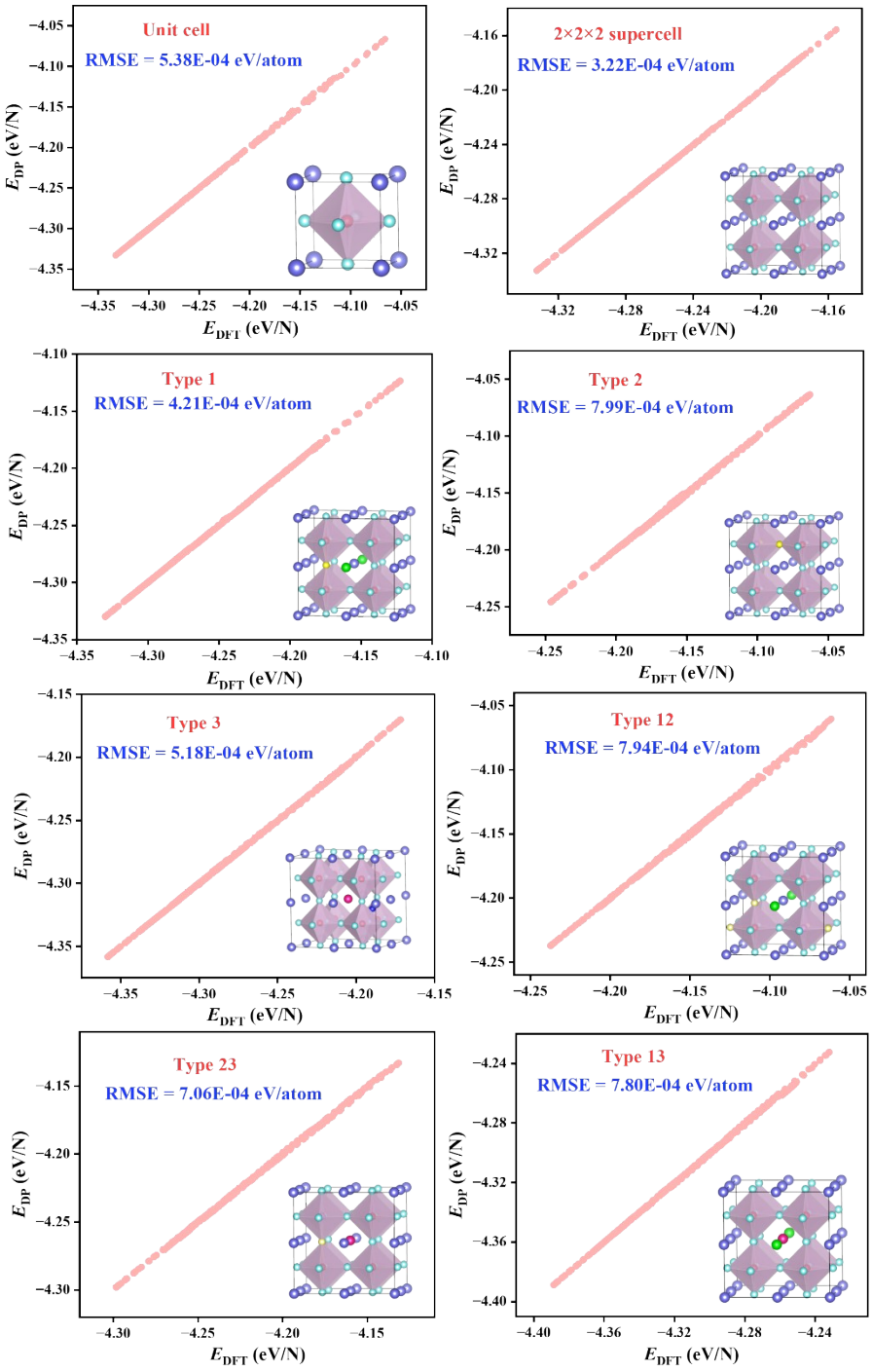

Figure S1. Energy comparison between DFT and DP calculations for Li_3OCl systems with different defects.

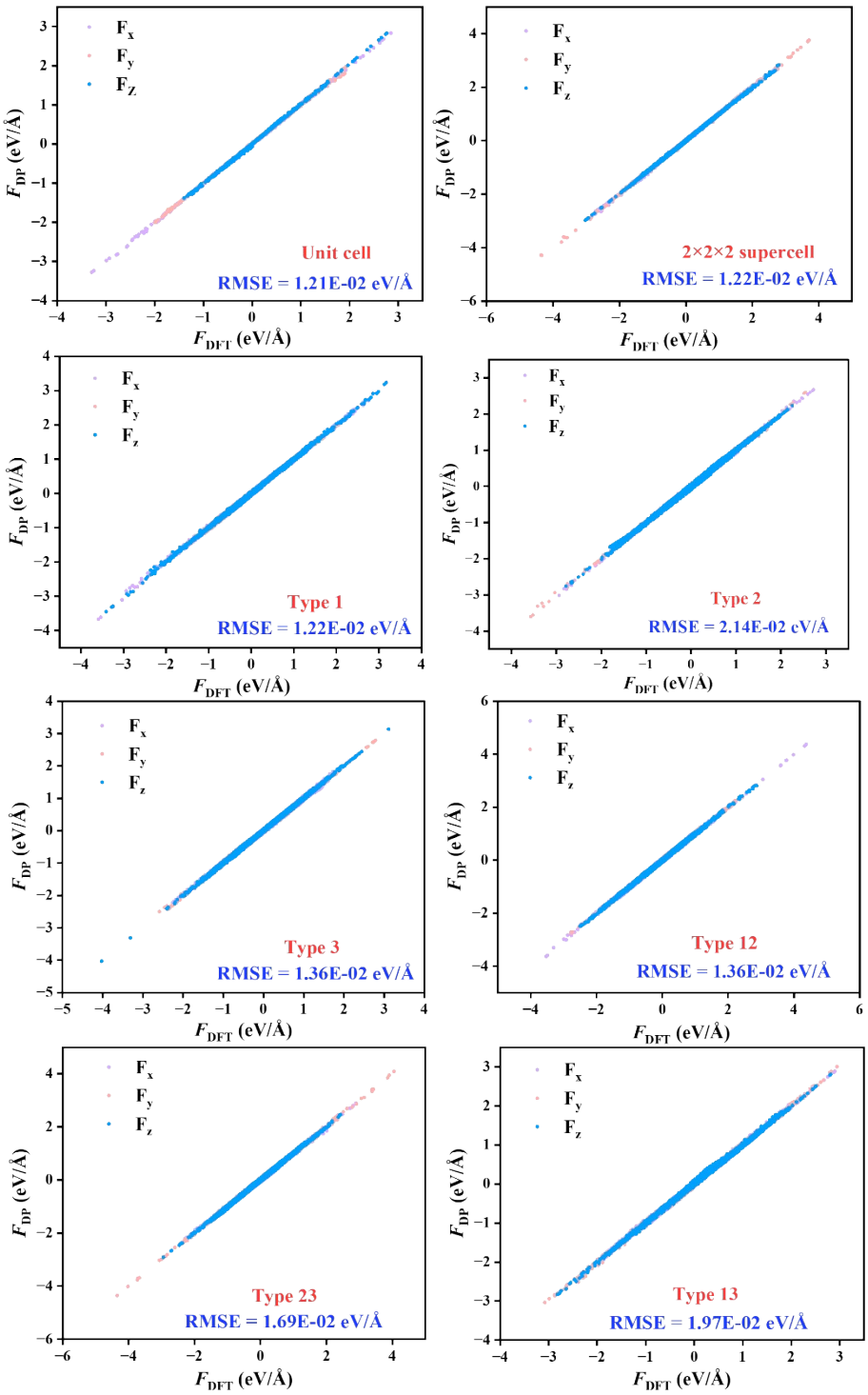

Figure S2. Force comparison between DFT and DP calculations for Li_3OCl systems with different defects.

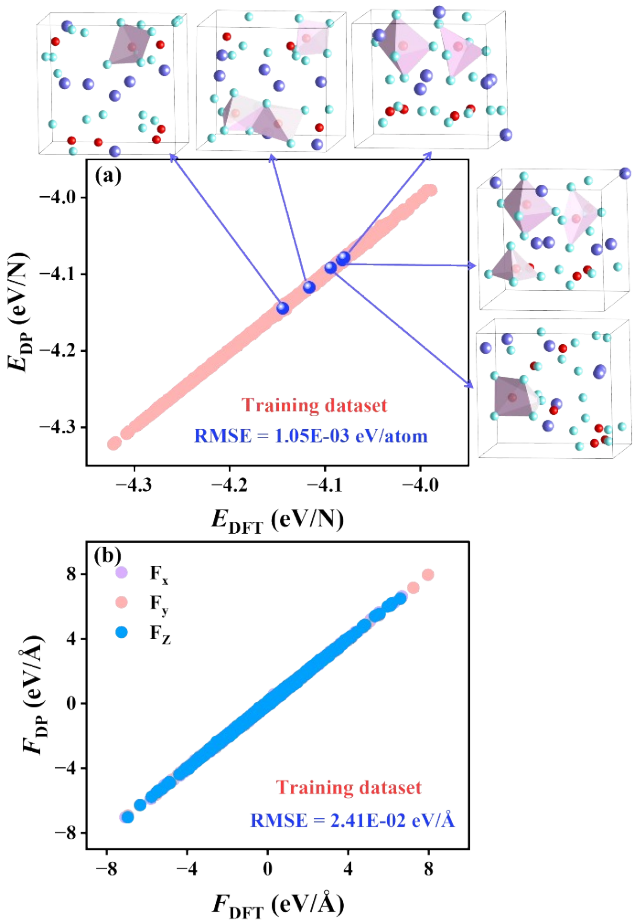

Figure S3. Comparison of energies and forces predicted by the DP model with DFT reference values for all configurations collected during DPGEN iterative sampling.

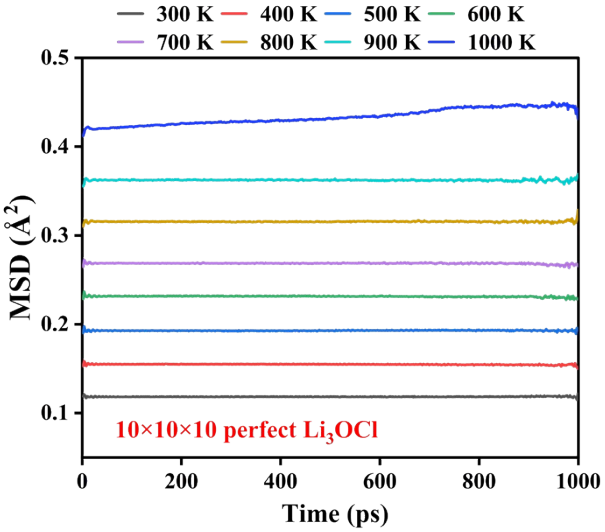

Figure S4. MSD curve of Li ion in 10×10×10 Li_3OCl with perfect structure.

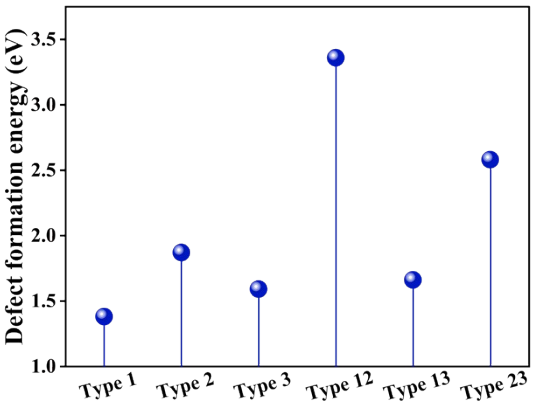

Figure S5. Formation energies of different types of defect pairs.

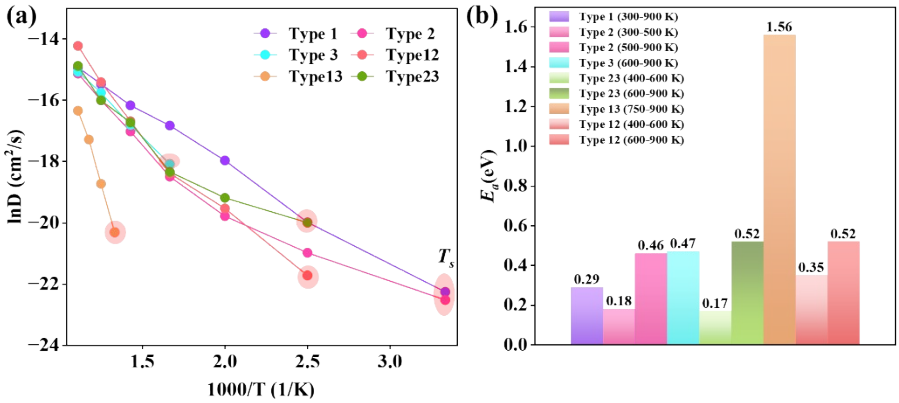

Figure S6. (a) Diffusion coefficients (T_s is circled in light red) and (b) activation energies of Li_3OCl systems containing different types of defects.

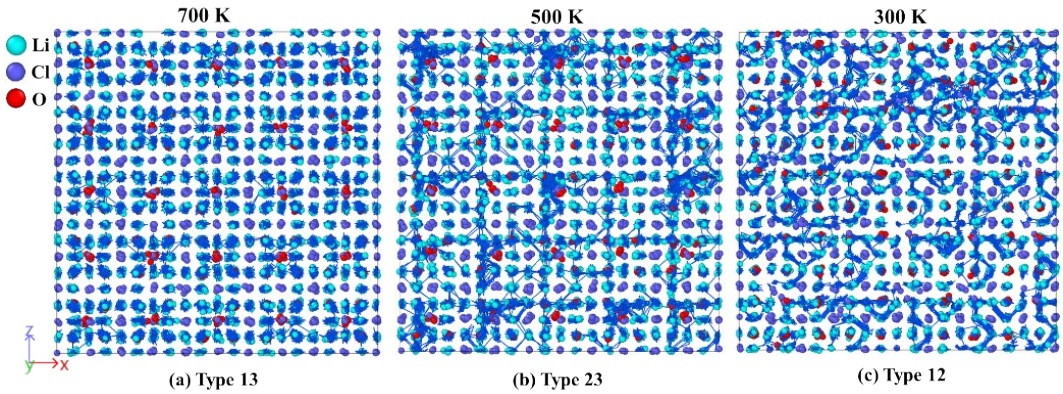

Figure S7. (a) Li ion diffusion trajectory of Type13 defect (b) Type23 composite defect (c) Type12 composite defect system after 1ns DPMD simulation.

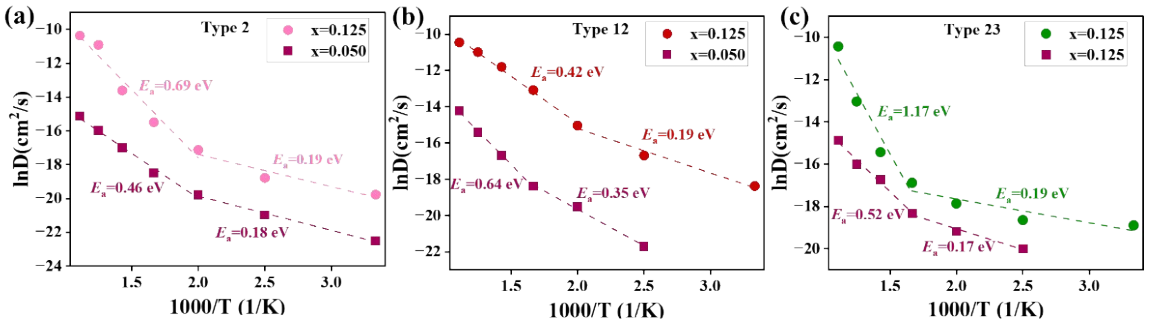

Figure S8. Diffusion coefficient as a function of temperature for the Li_3OCl system exhibiting non-Arrhenius behavior: (a) Type 2 ($Li_{3-2x}O_{1-x}Cl$), (b) Type 12 ($Li_{3-3x}O_{1-x}Cl_{1-x}$) (d) Type 23 ($Li_{3-x}OCl_{1-x}$).

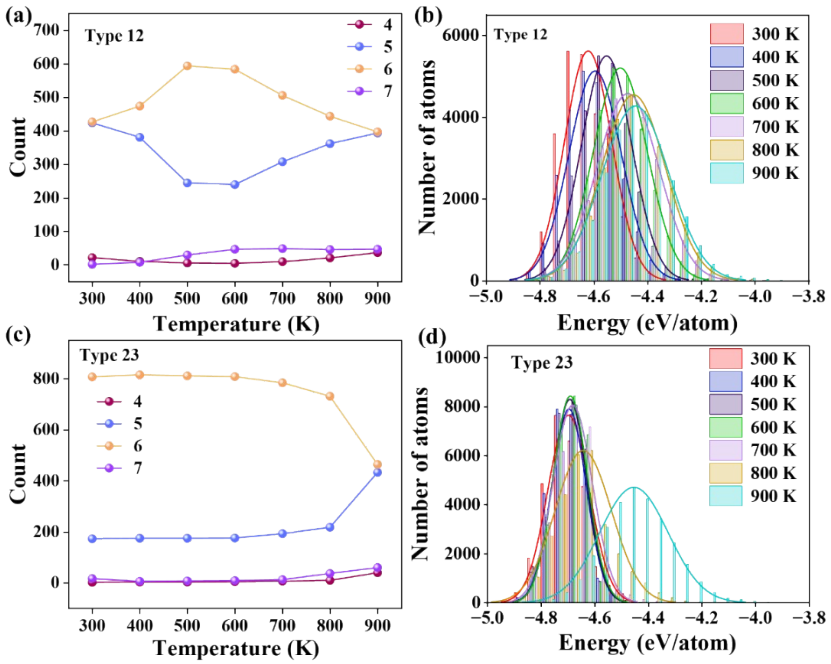

Figure S9. Type12 defect system: (a) The trend of the number of O-Li polyhedra changing with temperature (b) Energy distribution of lithium ions based on density of atomic states (DOAS) analysis. Type23 system: (c) The trend of the number of O-Li polyhedra changing with temperature (d) Energy distribution of lithium ions based on DOAS analysis.

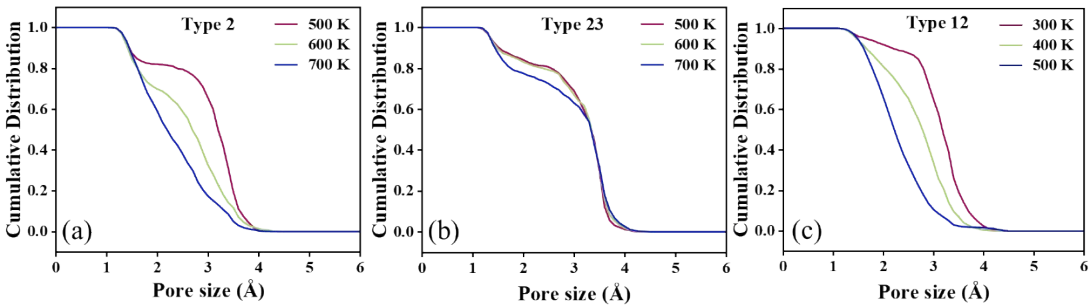

Figure S10. Cumulative distribution function of diffusion channels for different defect systems: (a) Type 2 defect system, (b) Type 23 defect system, (c) Type 12 defect system.

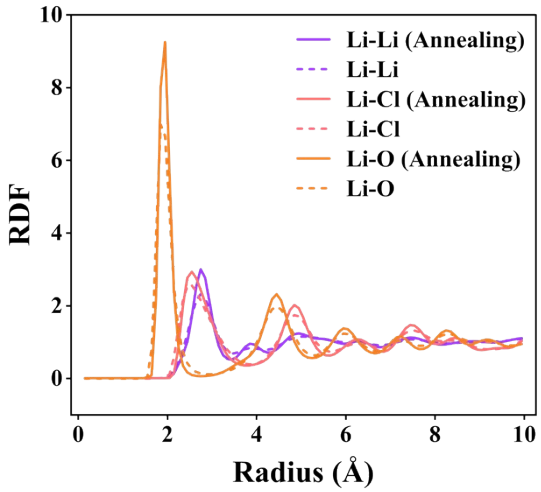

Figure S11. Comparison of radial distribution functions for Li-Li, Li-Cl, and Li-O pairs in the Type 2 defect system before and after annealing.

References

1 Z. Lu, C. Chen, Z. M. Baiyee, X. Chen, C. Niu and F. Ciucci, *Phys. Chem. Chem. Phys.,* 2015, **17**, 32547-32555.

2 J. Liu, R. wang, Y. Gao and Z. Zhong, *J. Alloys Compd.,* 2025, **1046**, 184679.